GLOW PEAK ANALYSIS OF PURE AND Ge-DOPED SILICA FLAT FIBER AT ULTRA HIGH DOSE ELECTRONS

ALAWIAH BINTI ARIFFIN

UNIVERSITI SAINS MALAYSIA

2015

GLOW PEAK ANALYSIS OF PURE AND Ge-DOPED SILICA FLAT FIBER AT ULTRA HIGH DOSE ELECTRONS

by

ALAWIAH BINTI ARIFFIN

Thesis submitted in fulfilment of the requirements

for the degree of

Doctor of Philosophy

JULY 2015

ACKNOWLEDGEMENT

Bismillahirrohmanirrohim. Alhamdulillah. I would like to take this opportunity to express my profound gratitude and deep regards to my supervisor, Associate Professor Dr Sabar Bauk (USM). I truly appreciate his exemplary guidance, monitoring and constant encouragement throughout the course of this research. Never forcing, always suggesting, suits me perfectly.

I would like to express my gratitude to Prof. David Bradley (Surrey University) and Prof. Hairul Azhar Abdul Rashid (Multimedia University) and, for their unflagging support and advice of one sort or another. Big thanks for their input and fruitful discussion on optical fiber matters. I would also like to thank the staffs of MCVD laboratory (TM R&D) for their advice and support in fiber fabrication matters, including Mr. Imran and Mr. Khairul.

It has been my privilege to work closely with Dr. Ghafour Mahdiraji Amauzad and Prof. Rafiq Adikan (Malaya University), I have enjoyed the opportunity to learn from their knowledge and experience in optical fiber and for bringing such an interesting problem to study, especially in this flat fiber dosimetry research. I would like to thank the My-Dosimetry Research Group Forum for an interesting discussion about optical fiber and providing an excellent cooperation throughout my research work.

I would also like to thank the technical staff of Alurtron, Nuclear Malaysia Agency, Malaysia, who actively involved during the irradiation task, which includes Mr. Zahidee, Mr. Shari, Mr. Azmi and Mr. Basit, for the technical set-up of an electron beam accelerator giving the ultra-high dose radiation. I would like to acknowledge Mr. Azizi and Dr. Wan Syafie for their technical support on the use of TLD reader

and other related equipment in Non-ionising Laboratory, Nuclear Malaysia Agency, Malaysia. Also, I want to thank the staffs of Medical Physics Group in Mount Miriam Cancer Hospital, Penang who made it possible for me to do experiments using LINAC facility for clinical radiotherapy dose range.

I would also like to thank all of my co-researchers, Dr. Noramaliza & Dr Nizam Tamchek (University Putra Malaysia), Dr. Marashdeh, KAST, Saudi Arabia and Dr. Gieszczyk, (INP, Poland) who supported me in writing, and stimulated me to strive towards my goal. Special thanks to my beloved lectures (Medical Physics & Physics); Prof. Mohamad Suhaimi Jaafar, Prof. Shukri Mustapa Kamal, Prof. Abd Aziz Tajuddin, Assoc. Prof. Wan Ahmad Kamil, Prof. Ahmad Zakaria, Assoc. Prof. Sivamany Kandaiya (University Sains Malaysia) and Tn. Haji Mohd Isa Mohd Yusoff (UiTM Puncak Alam), for their good influence then and since.

Words cannot express how grateful I am, to my mother, Hayati@Agnes Niun Bt. Abdullah and my father, Ariffin B. Harun. They have been a source of encouragement and inspiration to me throughout my life and very special thanks for providing me a ‘writing space’ and for nurturing me throughout the months of writing. They make me realized my potential and supported me to make this contribution to the world. Special thanks to my beloved kids; Syafiq, Farah, Aiman, Adam and Airil, for being so supportive and put up with the unavoidable side effects of doing PhD, even when being without mom was hard. This work is for, and because, all of them and all the generations to come. It is dedicated to their journeys in learning to thrive. At the end, I would like to express my appreciation to my beloved best friend, Karachi P. Turner, he has nurtured my learning, supported my dreams, who was always be my support in the moments when there was no one to answer my queries.

TABLE OF CONTENTS

CHAPTER 3: MATERIALS AND METHODS

CHAPTER 4: RESULTS AND DISCUSSION

LIST OF TABLES

LIST OF FIGURES

LIST OF ABBREVIATIONS

Name	Definition
AVD	Vapor Phase Axial Deposition
BCT	Burlin Cavity Theory
B-G	Bragg Gray
CPE	Charged Particle Equilibrium
CQ	Concentration Quenching
CRN	Continuous Random Network
CSDA	The continuous-slowing-down approximation range
ECC	Quality Factor
EDX	The Energy Dispersive X-ray Spectroscopy
EPR	Electron paramagnetic resonance spectroscopy
ERF	Energy Response Factor
FF	Flat Fiber
FOM	Figure of Merit
FWHM	Full Width Half Maximum
GCAFIT	Glow Curve Fit
GLPC	Germanium Lone Pair Center
Gy	Gray
HCP	Heavy Charged Particles
HTP	High Temperature Peak
HVL	Half Value Layer
IAEA TRS	International Atomic Energy Agency Technical Report Series

ICRP	International Commission on Radiation Protection
ICRU	International Commission on Radiation Units and Measurements
IMRT	Intensity Modulated Radiation Therapy
IPEM	Institute of Physics and Engineering in Medicine
ISO	International Standards Organization
KP	Kinetic Parameters
LC	Luminescence centers
LET	Linear Energy Transfer
LET	Linear energy transfer
LINAC	Linear Accelerator
LTP	Low Temperature Peak
MC	Monte Carlo
MCVD	Modified Chemical Vapour Deposition
MMF	Multi-Mode Fiber
MT	Maximum Temperature
N.A	Numerical Aperture
NBOHC	Non Bridging Oxygen Hole Center
NIST	National Institute of Standards and Technology
OA	Optical absorption
ODC	Oxygen deficient centers
OSL	Optically Stimulated Luminescence
OVD	Outside Vapour-Deposition
PCVD	Plasma Chemical Vapor Deposition
PHT	Pre-Heat Temperature

PI	Peak Integral
PL	Photoluminescence
PL	Photoluminescence
PMCVD	Plasma Modified Chemical Vapor Deposition
PMMA	Polymethyl Methacrylate
PMT	Photomultiplier Tube
QE	Quasi-equilibrium
R&D	Research and Development
R(E)	Energy Fit
RCFs	Reader Calibration Factors
RDD	Radial Distribution of Dose
RER	Relative Energy Response
RIA	Radiation Induced Attenuation
RIP	The Refractive Index Profile
ROI	Regions of Interest
RR	Relative Response
SEM	Scanning Electron Microscope
SEM-EDXRF	Scanning Electron Microscope Energy Dispersive X-ray Fluorescence
SIMM	Step-Index Multimode
SMF	Single-Mode Fiber
SSD	Source Surface Distance
SSDL	Secondary Standard Dosimetry Laboratory
TL	Thermoluminescence
TLD	Thermoluminescence Dosimeter

TPRs	Tissue-Phantom Ratio
TTP	Time-Temperature-Profile
UHD	Ultra-High Dose
UNIM	The Unified Interaction Model
UV	Ultra-violet
WinGCF	Windows Glow Curve Fit
WinREMS	Windows Radiation Evaluation and Management Software

LIST OF SYMBOLS

Name	Definition
SiO_2	Silica
E_a	Activation Energy
T_m *or* T_{max}	Maximum Peak Temperature
Ge	Germanium
E_g	Energy difference between the delocalised bands
T	Electron trap
R	Recombination Center
E_f	Fermi energy level
p	Probability per unit time
s	Frequency factor
$h\nu$	Radiant energy
E	Trap depth or activation energy
k	Boltzmann's constant
T_o	Initial temperature at equilibrium
$I(t)$	Photons per second
Im	Intensity at peak maximum
n_o *or* n_c	Concentration of free electron in the conduction band
m	Concentration of holes trapped at R
Am	Recombination probability
An	Retrapping probability
R	Non-radiative recombination center
β	Heating rate
μ_g	Geometry factor
ω	Full width on half maximum
δ	High temperature half width
n_1	Core refractive index
n_2	Cladding refractive index
θ_c	Critical angle

θ_A	Acceptance angle
$SiCl_4$	Silica Chloride
O_2	Oxygen
E'	Silicon dangling bond
f	Oscillator strength
S_o, S_1, T_1	Optical transition, ground state to singlet to triplet
g	Dosimeter's sensitive volume
μ_{en}/ρ	Mass-energy absorption coefficient
τ/ρ	Mass attenuation coefficient of photoelectric effect
τ_{tr}/ρ	Mass energy transfer coefficient
$S_E(D)$	Ratio of TL signal
$S'(E)$	Relative energy response
$\eta(E)$	Relative FF response to photons energy, E
$\mu'(E)$	Ratio of mass energy absorption coefficients
^{60}Co	Cobalt 60
$(dT/\rho dx)_{c,g}$	Mass collision stopping power
d	Cavity size
$\overline{D_g}$	Average absorbed dose
$D_w = (K_c)_w$	Absorbed dose in medium w (in water) under CPE conditions
${}_m\overline{S}_w^g$	Mean ratio of mass collision stopping powers for g and w
$\left(\frac{\overline{\mu_{en}}}{\rho}\right)_w^g$	Mean ratio of the mass energy-absorption coefficients for g and w
Z_{eff}	Effective atomic number
$a_1, a_2, a_3, \ldots\ldots a_n$	Weight fraction of each element in the fiber
$f(D)_{max}$	Maximum of TL efficiency (linearity index)
η	TL efficiency
$f(D)$	Linearity index

LIST OF PUBLICATIONS

Articles

In rev.	The thermoluminescence glow curve of Erbium doped silica fiber exposed to 70 kVp to 130 kVp of x-ray irradiation. *Applied Radiation and Isotopes*. Revise and resubmit stage.
In rev.	The effects of reader Time-Temperature-Profile (TTP) on thermoluminescence glow peaks of TLD-100 exposed to 6 MeV electrons using WinGCF. *Radiation Physics and Chemistry*. Revise and resubmit stage.
In rev.	Ultra-high dose thermoluminescence response of TLD-100 to 2.5 MeV electrons. *Radiation Physics and Chemistry*.
2015	Thermoluminescence glow curves and deconvoluted glow peaks of Ge doped flat fibers at ultra-high doses of electron radiation. *Radiation Physics and Chemistry*. 113, 53–58
2015	The thermoluminescence characteristics and the glow curves of Thulium doped silica fiber exposed to 10 MV photon and 21 MeV electron radiation. *Applied Radiation and Isotopes*. 98, 80–86
2015	Potential application of pure silica optical flat fibers for radiation therapy dosimetry. *Radiation Physics and Chemistry*. 106, 73–76

Proceedings

2013	Thermoluminescence characteristics of flat optical fiber in radiation dosimetry under different electron irradiation conditions. *Proc. SPIE 8775, Micro-structured and Specialty Optical Fibres II*, 87750S
2013	Assessment of GeB doped SiO_2 optical fiber for the application of remote radiation sensing system. *Proc. SPIE 8923, Micro/Nano Materials, Devices, and Systems*, 89235F

ANALISIS PUNCAK NYALA GENTIAN SILIKA TULIN DAN TERDOP Ge LEPER PADA DOS ELEKTRON ULTRA TINGGI

ABSTRAK

Gentian silika leper (FF), dicadangkan sebagai pengesan asas dan novel bagi pengukuran sinaran untuk pendarkilau haba (PH) yang dihasilkan. Kajian ditumpukan kepada kesan tindakbalas PH bagi sampel FF dan keluk nyala bagi PH. Pemecut Linear (LINAC) digunakan bagi dos dalam julat radioterapi di antara 0.2 Gy-10.0 Gy, manakala pemecut elektron digunakan bagi dos yang teramat tinggi dalam julat 1 kGy sehingga 1 MGy. Tindakbalas PH terhadap dos, kesan bahan dopan, kesan kadar pemanasan dan parameter kinetik PH adalah dikaji. Didapati keluk nyala bagi FF beralih kepada suhu yang lebih tinggi, dengan peningkatan kadar pemanasan. Parameter kinetik menunjukkan kebergantungan dengan kadar pemanasan, bagi kedua-dua jenis FF samada tulin atau terdop Ge. Juga didapati model tenaga, Teori Kaviti Burlin (BCT) boleh digunakan bagi meramalkan tindakbalas tenaga FF dengan tepat. Peningkatan bahan dopan daripada 0 wt % ke 6 wt % , didapati meningkatkan indek lineariti *f(D)* sebanyak 2 kali ganda. Kesan renjatan dopan dalam FF didapati bagi dopan 8 wt %. Kesan sensitiviti PH bagi 6 wt % Ge meningkat 3.5 kali ganda berbanding dengan silika tulin FF. Kesemua puncak lengkuk PH menunjukkan perilaku kinetik tahap pertama bagi julat dos di antara 0.1 – 10.0 Gy. Tahap maksimum supralinear bagi FF ialah pada ~30 kGy. Tiada penepuan berlaku pada $f(D)_{max}$. Peningkatan dos selepas tahap ini mengakibatkan pengurangan yang nyata bagi *f(D).* Perilaku PH sebelum tahap kritikal dos dicapai, dapat diterangkan oleh model kinetik PH, tetapi tiada model dapat menerangkan perilaku pelik PH bagi dos melebihi 10 kGy sehingga 1 MGy. Secara keseluruhannya FF berpotensi sebagai pengukur sinaran tahap dos elektron ultra tinggi.

GLOW PEAK ANALYSIS OF PURE AND Ge-DOPED SILICA FLAT FIBER AT ULTRA HIGH DOSE ELECTRONS

ABSTRACT

Silica flat fiber (FF) is being proposed as the basis for a novel radiation sensor of the thermoluminescence (TL) produced. The TL performance of the FFs and its respective glow curves were studied using a linear accelerator (LINAC) delivering doses of clinical radiotherapy within the range of 0.2-10.0 Gy. An electron accelerator (Alurtron®) was used to deliver the ultra-high dose. The TL dose response, dopant effect, heating rate effect and kinetic parameters of the deconvoluted glow peaks were investigated. The glow curve of FFs shifted to the higher temperature region as the heating rate increases. The kinetic parameters show dependence on the heating rate for both doped and un-doped FFs. It is found that the Burlin Cavity Theory (BCT) fit model can be used to predict the energy response of FF, accurately. Increasing the dopant concentration between 0 and 6 wt % Ge in FFs, increases the linearity index, $f(D)$ by 2.0. These remarkable findings showed the effect of dopant quenching in FF as the Ge dopant concentration was increased up to 8 wt%. The TL sensitivity of 6 wt% Ge doped FF was found to be 3.5 higher as compared to pure silica FF. Also noted, all peaks tend to show the first-order kinetics behavior within the linear dose range of 0.1 - 10 Gy. The maximum supralinearity of FFs found to be at ~30 kGy. No saturation occurred at $f(D)_{max}$ and further increases of dose up to 1 MGy, exhibits a significant decrease in *f(D)*. The TL kinetic model can be used to explain the TL glow peak before the critical dose limit was achieved whereas none of TL model can explain the strange changes in TL glow peak at doses > 10 kGy up to 1 MGy. Overall results indicate that the silica FFs have a considerable potential as radiation sensors in ultra-high dose electrons.

CHAPTER 1: INTRODUCTION

1.1 Research background

Thermoluminescence (TL) dosimetry is a well-known method applied in radiation dose measurement especially in the area of personnel, medical and environmental dosimetry. The micro spatial resolution, TL sensitivity, TL fading, reproducibility, flexibility, product cost, ease of use and TL response in the dynamic dose range (high field gradient), are the challenges of any radiation dosimetry system. There are the needs of more efficient, more reliable, more accurate and more sensitive, TL material especially in improving the clinical outcome of any radiation therapy modality.

Currently, several dosimetry research groups all over the world have revealed the remarkable potential of the silica (SiO_2) optical fiber to be used as a TL radiation detector. They are strongly confident of being able to overcome the shortcomings of the widely used TLD-100 dosimeter, both in clinical (radiation therapy) and non-clinical (food irradiation and environmental dose monitoring) dosimetry applications. This is a new direction for medical research on dosimetry and radiation therapy procedure and is a promising cutting edge technology in medical radiation as well as in global radiation monitoring modality.

The considerable potential of silica (SiO_2) optical fibers as a new TL material in dosimetry, has attracted much attention as a radiation sensor in dosimetry which can be found in a number of reports (Hashim et al., 2009; Ong et al., 2009; Issa et al., 2011; Alawiah et al., 2014; Alawiah et al., 2013). Many studies have been carried out to improve its TL sensitivity as well as to develop new TL model for the new TL material. Different types of radiation has been used in TL research of this fiber such as X-rays, synchrotron microbeam, electron linear accelerators (LINAC), protons, neutrons and alpha particles, which were also covered within the wide range of dose between μGy up to kGy (Abdulla et al., 2001; Ramli et al., 2009; Hashim et al., 2010; Yusuf et al., 2005; Noor et al., 2010, 2011; Abdul Rahman et al., 2010a, 2010b, 2011; Alawiah et al., 2013, 2015). It was recently revealed that pure SiO_2 flat fiber (FFs) can be used as radiation sensors in the medical therapy dosimetry within the dose range of 0.1 – 10 Gy (Alawiah et al., 2015) and the FFs showed 16% higher sensitivity as compared to the TLD-100 (Hashim et al., 2015).

Other benefits of silica fiber revealed by Espinosa et al. (2006) who used the commercial SiO_2 optical fiber manufactured by Nokia Cable®, with 150 μm diameter and found that the optical fiber presents 1.3 times more TL signal than the LiF for the same dose of 10 Gy. The fiber shows a linear TL response within the dose range of 0.1 – 3 Gy, which is can be beneficial for clinical radiation dosimetry. Epinosa et al. (2006) also found that the fiber demonstrated high reproducibility, low residual signal, low fading and can be re-used without any loss in the TL dose response. All these TL characteristics, plus the small size of the fiber, the high flexibility, easy handling and low cost compared with other TL materials, make the

commercial optical fiber a very promising TL material for use in research, medicine, industry, reactors, and a variety of other applications.

The commercially available Al- and Ge-doped optical showed linear dose response to doses ranging from 0.2 to 4.0 Gy of 6, 9 and 12 MeV electron beams (Yaakob et al., 2011). Yusoff et al., (2005) found that the 4.0 mol % aluminium-doped silica provides ~3.5 times higher TL yield as compared to TLD-100 and ~5.4 times higher as compared to the germanium-doped silica fiber. The Ge-doped fibres offering a response of 59 % higher as compared to TLD-100 (Wagiran et al., 2012)

High dose radiation has attracted much attention as increasing needs in food irradiation industry, radiation protection on an extreme dose field and nuclear reactor dose monitoring. Widely used LiF based TL material such as TLD-100 has a limitiation on its sensitivity while dealing in with an extremely high dose environment, known as ultra-high dose (UHD) radiation. TLD-100 tends to show a significant reduction of TL sensitivity following irradiation dose greater than 10 kGy. Bilski et al. (2008a) found that TLD-100 loses their sensitivity to a large extent as a result of UHD radiation and exhibited a saturation of TL response within the dose range of 10 – 50 kGy (Bilski et al., 2010). The SiO_2 optical fiber that is proposed in this research is strongly confident of being able to overcome such shortcomings.

1.2 Research motivation

This study intends to investigate the TL response and the sensitivity of SiO_2 optical fiber, mainly the flat fiber (FF) shape type, at doses at much higher than 1 kGy and can be up to 1 MGy of radiation dose, since the study of the TL response of the SiO_2 optical fiber at ultra-high dose (UHD) is very scarce. It is also need to investigate the shape of the TL glow curve of SiO_2 FF samples, evaluate the changes in TL supralinearity during UHD radiation, and to explain the experimentally observed TL glow curves and the deconvoluted glow peaks using the existing TL models. The effect of dopant, radiation energy, radiation dose and heating rate, on the kinetic parameters of the deconvoluted glow peaks will also be studied.

The TL characterisation of SiO_2 optical fiber materials requires detailed analysis of the TL glow curve and the kinetics parameters of its individual glow peaks. It is also intends to evaluate the TL glow curve response by Windows Radiation Evaluation Management Software (WinREMS) and determine its kinetic parameters by Windows Glow Curve Fit (WinGCF) deconvoluted glow peak for the UHD region of interest. TL glow curves were deconvoluted into single first-order peaks by using the WinGCF program.

1.3 Problem statement

The radiation sensor sensitivity is one of the primary challenges facing radiation protection dosimetry in recent decades. Both the clinical and environmental sectors have hastened to respond to emerging needs of the accuracy and sensitivity in radiation detection and measurement. Scholars in many fields have addressed these important inquiries. Over many types of new radiation sensor materials have been developed in recent years (Issa et al., 2011; Ong et al., 2009). Within thermoluminescence (TL) dosimetry, scholars such as Bradley et al. (2014), Hashim et al. (2009), and Yusoff et al. (2005) have all explored the role of silica fiber as a radiation sensor in both, clinical and environmental radiation monitoring applications. Within optical sensor studies, meanwhile, scholars such as Noor et al. (2014), Begum et al. (2013), and Paul et al. (2007) have focused on the specific dopant material and geometrical shape which have enhanced the sensor sensitivity.

However, scholars in these fields have not yet adequately addressed the limitation of TL response of the pure and Ge-doped silica flat fiber at ultra-high doses of electron radiation. Despite much excellent work on TL such as dose linearity response and TL glow curve, scholars examining the TL glow curve behavior, have not yet fully explored the importance of dopant concentration, supralinearity response and critical dose limit, in ultra-high dose radiation field. Yet, without such an understanding, this field is left with an inadequate analysis that creates the condition for misinterpretation of the TL glow curve and main dosimetric peak evaluation and improper of kinetic model implementation.

This study will remedy these gaps in the literature by examining the TL glow curve response and determine the supralinearity response and the critical dose limit of pure and Ge-doped silica flat fiber, in order to more fully elucidate the heretofore unrecognized relationships between the kinetic parameters and the supralinearity behavior at the specifically high dose electrons radiation field.

Through a close and fine-grained analysis of the TL glow curve and its supralinearity behavior, this study will show that in contrast to previous assumptions in TL model, in fact TL glow curve response of pure and Ge-doped silica flat fiber is not saturated at high dose electrons radiation. It is expected that this study to contribute to debates on the TL glow curve response and play an important role in shaping debates on the limitation of TL models and supralinearity behaviour of silica flat fiber in the coming years.

1.4 Objectives

Main Objective:

To evaluate and analyze the TL properties of the silica flat fibers (FF) as a potential of a new TL dosimeters at the ultra-high dose (UHD) electrons radiation.

Specific Objectives

1) To determine the main dosimetric peak of FF.
2) To characterize the TL glow curve behavior at UHD radiation in response to different dopant concentration.
3) To determine the maximum dose limit of FF at UHD radiation
4) To investigate the supralinearity behavior of FF at UHD radiation.
5) To evaluate the TL kinetic parameters of FF at UHD radiation.

1.5 Scope of research

The scope of this research is stated as per following:

- The effect of heating rate on the dosimetric properties of TL response of FF and its glow curve
- The effect of irradiation energy on FF and energy response model evaluation
- The effects of Germanium dopants on TL dosimetric properties and glow curve
- The effect of radiation dose on kinetic parameters of the FF and main dosimetric peak determination by deconvoluted glow peak.

1.6 Thesis outline

Following the interest in this field, this thesis deals with the experimental study of the TL dosimetric properties and the glow curve response of three types of SiO_2 FF and TLD-100 following wide range of irradiation dose, which covered in therapeutic dose range and extremely high dose radiation of electron. The samples have been designed and fabricated to investigate the role of Germanium (Ge) dopant element on the TL response and eventually on the radiation sensitivity of silica fiber based, as the potential of new radiation dosimeter. The characterisation of the TL behaviours of these fiber samples following irradiation within the range of 0.1 Gy, up to 1 MGy, through the selected curve fitting techniques, to obtain the kinetic parameters information which includes; the activation energy, E_a, the maximum peak temperature, T_{max} and the peak integral, PI.

The thesis is organized in five chapters. Chapters 1 and 2 deal with the research background and literature review of optical fiber in radiation sensory system of clinical and environmental dosimetry providing an extensive overview of the thermoluminescence (TL) principle, the TL kinetic model and benefits of optical fiber, with particular emphasis on the importance of the dopant concentration to enhance the TL response and sensitivity of SiO_2 fiber dosimetric characteristics. An overview of the basic structure of silica fiber, type of fiber, and the main intrinsic and extrinsic defects in silica are also presented.

Chapter 3 is devoted to the description of the type samples used in this study and of the adopted experimental techniques and specific methodology. Chapter 4 reports on the heating rate experiments, on the pure and Ge-doped FF samples and their main TL glow curve results and evaluation of its kinetic parameters. This chapter also reports on the effect of radiation energy to TL glow curve response of FF and discusses the most relevant energy model for explaining the experimental results. Chapter 4 is devoted to reveal the effect of dose on FF, with more emphasize on the ultra-high dose range of electrons. The experimental results concerning with the dose response behavior (linear and supralinear), the maximum dose limit, the sensitivity, the evaluation of kinetic parameters and TL kinetic model, are thoroughly discussed. In Chapter 5, finally, the most relevant conclusions are summarized. A list of the scientific papers comprising the results presented in this thesis (refer to the List of publication) and a few others on closely related topics are reported at the end of this thesis, together with a list of communications in conferences.

CHAPTER 2: THEORY AND LITERATURE REVIEW

2.1 Introduction

A thermoluminescent material absorbs radiant energy during irradiation exposure and stored the energy in the material. The stored energy is then released in the form of luminescence light which is visible, when the material is heated. The purpose of this Chapter is to highlight the basic concepts of thermoluminescence (TL) with its applications in dosimetric systems.

The TL concept will be discussed by using a simple model of the TL mechanism, which forms the basis of the TL theories in material. TL model is used to interpret the experimental observation of TL response with regards to dose response, energy response, TL materials, TL sensitivity, TL fading and many other dosimetric TL responses.

The TL model also being used for the evaluation of TL kinetic parameters which includes the activation energy, E_a, the maximum peak temperature, T_{max} and peak integral, PI of an individual TL glow peak.

2.2 The one trap and one recombination center model (OTOR)

The energy band theory can be used to explain the TL properties of solid. In the equilibrium state, most of the electrons are located in the valence band. The electrons can be excited to the conduction band, which is separated by the forbidden band gap and the valence band, with the energy difference of E_g. However, electrons can have forbidden energies, when there are structural defects or impurities within the lattice structure of the solid material.

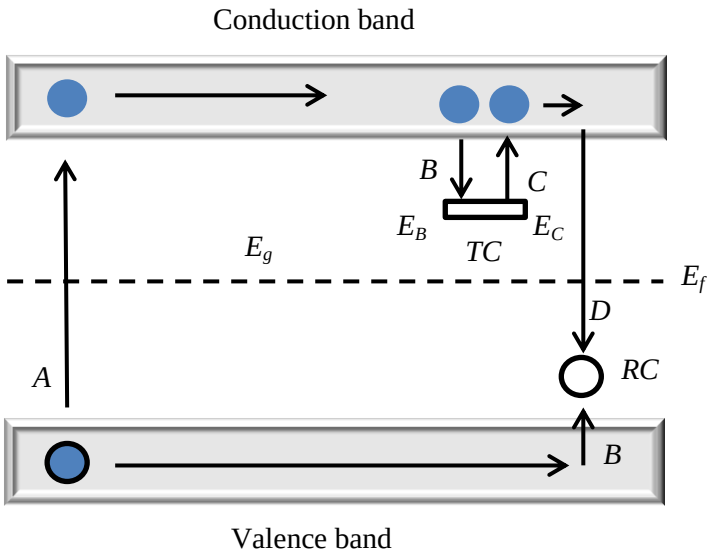

Figure 2.1: OTOR model of electron-hole transitions in a TL material. Transition (A) showing the generation of electrons and holes; (B) electron and hole trapping; (C) release of electron from the electron trap (*TC*) due to thermal stimulation; (D) electron recombines with hole at the recombination center (*RC*). Solid circles are electrons, open circles are holes. *TC* is an electron trap energy level (E_B and E_C), *RC* is a recombination centre, E_f is Fermi energy level and E_g is the band gap energy level.

Two levels are assumed, which are *TC* and *RC* as shown in **Figure 2.1**. *TC* is a potential trap for electron, which is situated below the bottom of the conduction band (above the Fermi energy level, E_f) and *RC* is at the above the top of the valence band. The *TC* is being emptied during the equilibrium state.

On the other hand, *RC* is a potential trap for the hole, migrates from the valence band after the occurrence of transition A. *RC* is known as the recombination centre for electron and hole. When the incident radiation energy exceeds the band gap energy level as $h\nu > E_g$, producing free electrons (by ionization process) and holes. The electrons will move freely in the conduction band before being captured by the electron trap (*TC*) which located near the conduction band in the forbidden gap.

On the other hand, the hole in the valence band will move freely, before being captured by the hole trap (*RC*) located near the valence band in the forbidden gap. After thermal energy absorption, the electrons were released from its trap (*TC*), move back to the conduction band and then recombine with the hole at the recombination center (*RC*), with a release of luminescence light.

The Arrhenius equation is used to express the probability of release of an electron from the trap per unit time, as in **Eq. (2.1)**.

$$p = s \exp\left[-\frac{E_c}{kT}\right] \qquad \text{(Eq. 2.1)}$$

where p is the probability per unit time. The term s is called the frequency factor or attempt to escape factor. In the OTOR model, s is temperature independent and considered as a constant, known as the lattice vibration frequency, of range 10^{12} – 10^{14} s^{-1}. E_C , known as the activation energy to release an electron from the trap into the conduction band. k = Boltzmann's constant = 8.617×10^{-5} eV K^{-1}, and T the absolute temperature.

When the trap depth, $E_C >> kT_o$, with T_o the initial temperature during irradiation, then any trapped electron will remain in *TC*. Free electrons and holes are created with the condition of an equal population.

When the temperature of the TL material raising above T_o, the electrons will be released from *TC* to the conduction band and thus the probability of de-trapping decreases. The electrons will then recombine with the holes at the recombination centre *RC*, producing the luminescence light, which is known as thermoluminescence (TL).

The TL intensity is proportional to the rate of recombination of holes and electrons at *RC*. If m (m^{-3}) is the concentration of holes trapped at *RC* the TL intensity, *I(t)* can be written as in **Eq. (2.2)**.

$$I(t) = -\frac{dm}{dt} \qquad \text{(Eq. 2.2)}$$

where the negative sign indicates a decrease of holes.

In the OTOR model, it is assumed that, each recombination transition, produces luminescence light which then being measured of its intensity. The rate of recombination is proportional to the concentration of free electrons in the conduction band n_c and the concentration of holes m in the recombination center, as in **Eq. (2.3)**.

$$I(t) = -\frac{\mathrm{d}m}{\mathrm{d}t} = n_c m A_m \qquad \text{(Eq. 2.3)}$$

with the constant A_m is the recombination probability expressed in units of volume per unit time which is to be independent of the temperature.

The concentration rate of trapped electrons n is equal to the rate of thermal release, minus the rate of retrapping, as in **Eq. (2.4)**.

$$-\frac{\mathrm{d}n}{\mathrm{d}t} = np - n_c(N-n)A_n \qquad \text{(Eq. 2.4)}$$

with N the concentration of electron traps and A_n the probability of retrapping ($m^3 s^{-1}$) The concentration rate of free electrons is equal to the thermal release rate, minus the re-trapping rate and the recombination rate, as written in **Eq. (2.5)**.

$$\frac{\mathrm{d}n_c}{\mathrm{d}t} = np - n_c(N-n)A_n - n_c m A_m \qquad \text{(Eq. 2.5)}$$

The TL intensity produced by the recombination at RC, is given by **Eq. (2.3)**. The traffic of the charge carrier traffic, expressed by **Eqs. (2.3 – 2.5)**, in the case of release of a trapped electron from *TC* and recombine with hole in *RC*.

Eq. 2.6 is the quasi equilibrium (QE) assumption by Chen and McKeever, (1997), at its quasi stationary state and can be written as,

$$\left|\frac{\mathrm{d}n_c}{\mathrm{d}t}\right| << \left|\frac{\mathrm{d}n}{\mathrm{d}t}\right|; \quad \left|\frac{\mathrm{d}n_c}{\mathrm{d}t}\right| << \left|\frac{\mathrm{d}m}{\mathrm{d}t}\right| \qquad \text{(Eq. 2.6)}$$

The free electrons and holes are produced in pairs from transition *A*, therefore:

$$n_c + n = m \qquad \text{(Eq. 2.7)}$$

When $n_c \approx 0$, then $n \approx m$, thus

$$I(t) = -\frac{\mathrm{d}m}{\mathrm{d}t} \approx -\frac{\mathrm{d}n}{\mathrm{d}t} \qquad \text{(Eq. 2.8)}$$

At $\mathrm{d}n_c/\mathrm{d}t \approx 0$, then from **Eqs. (2.5)** and **(2.6)**

$$I(t) = \frac{mA_m ns \exp\left\{-\frac{E}{kT}\right\}}{(N-n)A_n + mA_m} \qquad \text{(Eq. 2.9)}$$

2.3 TL Kinetic Model

2.3.1. First-order kinetics

Randall and Wilkins (1945a, b) assumed no re-trapping during the heating stage, and assumed that, $mA_m >> (N-n)A_n$. Therefore **Eq. (2.9)** can be written as

$$I(t) = -\frac{\mathrm{d}n}{\mathrm{d}t} = sn\exp\left\{-\frac{E}{kT}\right\} \qquad \text{(Eq. 2.10)}$$

Eq. (2.11) describes the charge transport in the lattice as a first-order process. If the temperature is kept constant, $p = s\exp(E/kT)$ and the intensity is given by the following equation.

$$I(t) = I_o \exp(-tp) \qquad \text{(Eq. 2.11)}$$

where I_o is the initial TL intensity at time $t = 0$. When temperature varies in time, p is no longer a constant and therefore **Eq. (2.10)** becomes as **Eq. (2.12)**.

$$I(t) = -\frac{dn}{dt} = n_o s\exp\left\{-\frac{E}{kT(t)}\right\} \mathrm{x}\exp\left\{-s\int_0^t\left\{-\frac{E}{kT(t')}\right\}dt'\right\} \qquad \text{(Eq. 2.12)}$$

where n_0 is the total number of trapped electrons at $t = 0$.

As the temperature increases, the TL intensity initially increases, than reach a maximum and finally decreases. **Eq. (2.10)** is called a first-order glow peak. The TL intensity is observed as the temperature is raised within the linear function of time as shown in **Eq. (2.13)**.

$$T(t) = T_o + \beta t \qquad \text{(Eq. 2.13)}$$

with β is the heating rate and T_o is the temperature at $t = 0$.

The TL intensity as function of temperature is given by **Eq. (2.14)**.

$$I(T) = -\frac{1}{\beta}\frac{\mathrm{d}n}{\mathrm{d}t} = n_o \frac{s}{\beta}\exp\left\{-\frac{E}{kT}\right\} \mathrm{x} \exp\left\{-\frac{s}{\beta}\int_{T_o}^{T}\left\{-\frac{E}{kT'}\right\}dT'\right\} \qquad \text{(Eq. 2.14)}$$

This equation is known as the Randall–Wilkins first-order kinetic.

The asymmetric shape peak is wider on the low temperature region of glow curve as compared to the high temperature region.

Halperin and Braner (1960) defined a geometry factor $\mu_g = \delta/\omega$ with δ is the high temperature half width and ω is the full width at half maximum (see **Figure 2.2**).

I is plotted as function of 1/*T* and a straight line is expected with the slope of −*E*/*k*.

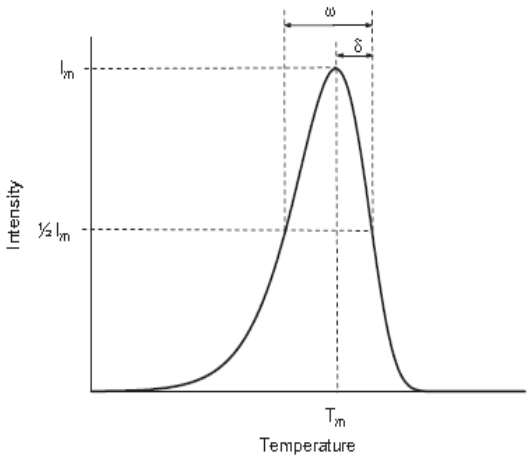

Figure 2.2: The typical glow peak (normalized) which is based on the Randall and Wilkins first-order TL kinetic (**Eq. (2.14)**). The asymmetry or geometry factor μ_g defined as $\mu_g = \delta/\omega$. (After Bos, 2007)

The properties of the Randall and Wilkins, **Eq. (2.14)** are illustrated in **Figure 2.3** with the following constant parameters values; n_0 = 0.25 m $^{-3}$ till n_0 = 2 m $^{-3}$ while E = 1 eV, s = 1.0×10^{12} s $^{-1}$ and β = 1 K/s.

The main characteristic of the first-order TL glow curves is that the maximum peak temperature, T_m, remain unchanged, as in **Eq. (2.15)**.

$$\frac{\beta E}{kT_m^2} = s\exp\left\{-\frac{E}{kT_m}\right\} \qquad \text{(Eq. 2.15)}$$

For a given E and s the peak maximum can be found by the following **Eq. (2.16)**.

$$T_{m,new} = \frac{E}{k}\left[\ln\left(\frac{sk}{\beta E}T_{m,old}^2\right)\right]^{-1} \qquad \text{(Eq. 2.16)}$$

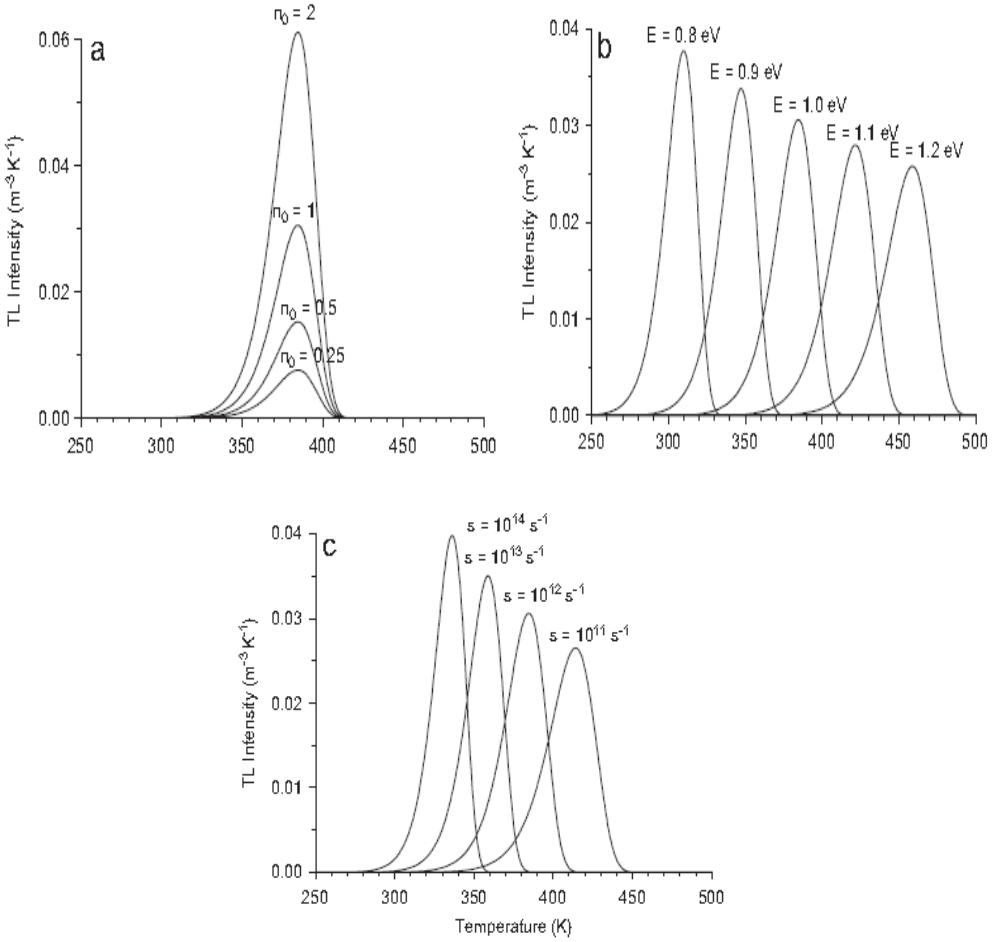

Figure 2.3: Typical Randall and Wilkins first-order TL glow curve showing: (a) the effect of the concentration of trapped charge carriers after irradiation n_0; (b) the effect of the activation energy E; (c) the effect of escape frequency s. (After Bos, 2007)

Figure 2.3 (a) shows that at each point of the curve is proportional to n_0. The n_0 is the parameter that is proportional to the absorbed dose. The area under the glow peak is equal to n_0 since in **Eq. (2.17).**

$$\int_0^{\infty} I(t)\,\mathrm{d}t = -\int_0^{\infty} \frac{\mathrm{d}n}{\mathrm{d}t}\,\mathrm{d}t = -\int_{n_o}^{n_\infty} \mathrm{d}n = n_o - n_\infty \qquad \text{(Eq. 2.17)}$$

and n_∞ is zero for $t \to \infty$.

Shown in **Figure 2.3(b),** the activation energy E has been varied from 0.8 to 1.2 eV. As the E increases, the peak shifts to much higher temperatures with a decrease in glow curve height and an increase in the width of glow curve, but instead keeping the area constant.

The shift to higher temperatures observed, because for the higher E values (deeper traps) more energy (higher temperature) is needed to release the charge carriers.

At **Figure 2.3(c)**, as s increases the peak shifts to lower temperatures with an increase of the height and a decrease in width. This is because, a high frequency factor needs less energy (lower temperature) to free a charge carrier.

The TL intensity at the peak maximum, derived by Hoogenboom et al. (1988), is given by **Eq. (2.18)**.

$$I_m = n_o \frac{\beta E}{kT_m^2} e^{-g_m} \qquad \text{(Eq. 2.18)}$$

with $g_m = g(x) = xe^x E_2(x)$ with $E_2(x)$ the exponential integral of second-order and $x = E/kT_m$. At g_m = 1 the I_m increases up to 10%. From **Eq. (2.18)**, the peak height is proportional to n_0 and the heating rate β and is illustrated in **Figure 2.4 (a)**. The peak area and the asymmetry remain the same as the heating rate changes.

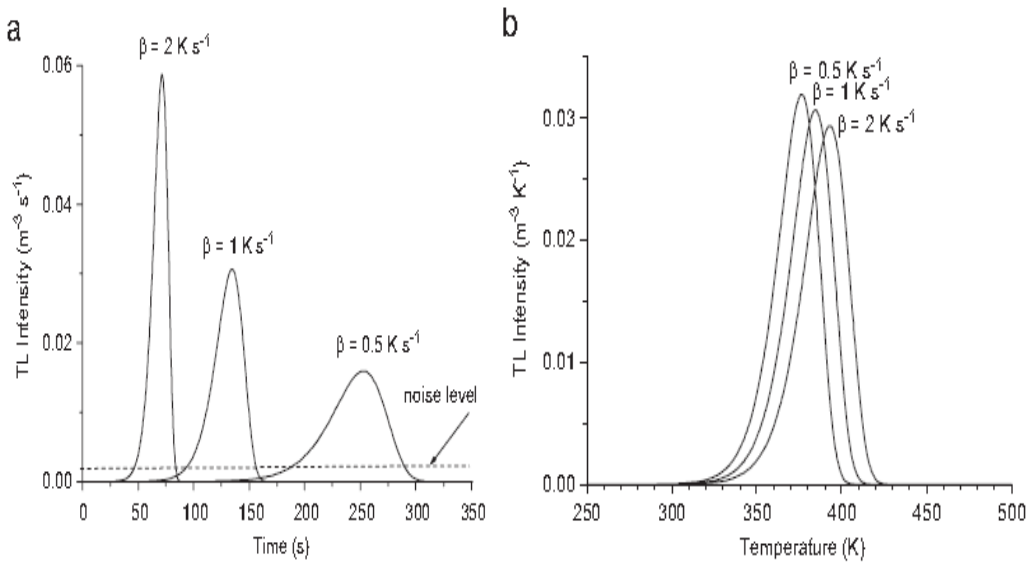

Figure 2.4: Effect of the heating rate β on the Randal and Wilkins first order glow curve. (a) The TL intensity is plotted as a function of time (b) The TL intensity is plotted as a function of temperature. Parameter values: n_0 = 1 m $^{-3}$; E = 1 eV; s = 1 x 10^{12} s $^{-1}$ (After Bos, 2007)

The signal to noise ratio is reduced at higher heating rate as shown in **Figure 2.4(a),** but instead for a low heating rate, the noise is produced for a much longer time.

The TL intensity is plotted as function of temperature as shown in **Figure 2.4(b)**. As the heating rate increases, the peak shifts to higher temperatures while the peak height decreases and the glow peak width increases.

By using the varying heating rate method, introduced by Hoogenstraten (1958), plotting $\ln\left(\beta/T_m^2\right)$ as a function of 1 / T_m, produces a straight line and E can be determined from the slope.

Meanwhile, the Quasi-equilibrium (QE) assumption has been evaluated by Sunta et al. (2002), based on changes of the geometry factor μ_g of the glow peak measured at different heating rates, and found that the QE assumption system will show a symmetry glow peak that is independent with heating rate.

For a new TL material, it is important to investigate the effect of glow peak with the variation of the heating rate, radiation dose, radiation energy and dopant concentration in a material. The TL properties which are related to the trapping center, include the activation energy E, the maximum peak temperature, T_{max} and peak integral, PI. Experimentally, the TL intensity of the peak maximum is denoted as I_m and the temperature at the maximum is T_m.

Kitis et al. (1998) found the expression that may be suitable for peak fitting purposes as in **Eq. (2.19)**.

$$I(T) = I_m \exp\left[1 + \frac{E}{kT}\frac{T - T_m}{T_m} - \frac{T^2}{T_m^2} x \exp\left\{\frac{E}{kT}\frac{T - T_m}{T_m}\right\}(1 - \Delta) - \Delta m\right] \qquad \text{(Eq. 2.19)}$$

with $\Delta = 2kT/E$ and $\Delta_m = 2kT_m/E$.

2.3.2. Second-order kinetics

Garlick and Gibson (1948) considered the possibility that retrapping dominates as $mA_m << (N - n)A_n$ and also assume less saturation for $N << n$ and $n = m$. These assumptions makes **Eq. (2.19)** becomes as **Eq. (2.20)**.

$$I(t) = -\frac{\mathrm{d}n}{\mathrm{d}t} = s\frac{A_m}{NA_n} n^2 \exp\left\{-\frac{E}{kT}\right\} \qquad \text{(Eq. 2.20)}$$

The rate of dn/dt is proportional to n^2, which produces a second-order reaction. Applying an additional assumption of equal probabilities of recombination and retrapping, $A_m = A_n$, **Eq. (2.20)** can be solved in terms of second order as

$$I(t) = \frac{I_o}{(1 + n_o \alpha t)^2} \qquad \text{(Eq. 2.21)}$$